

Asymptotic reductions and solitons of nonlocal nonlinear Schrödinger equations

Theodoros P. Horikis¹, Dimitrios J. Frantzeskakis²

¹Department of Mathematics, University of Ioannina, Ioannina 45110, Greece

²Department of Physics, National and Kapodistrian University of Athens, Panepistimiopolis, Zografos, Athens 15784, Greece

E-mail: horikis@uoi.gr

Abstract. Asymptotic reductions of a defocusing nonlocal nonlinear Schrödinger model in $(3+1)$ -dimensions, in both Cartesian and cylindrical geometry, are presented. First, at an intermediate stage, a Boussinesq equation is derived, and then its far-field, in the form of a variety of Kadomtsev-Petviashvili (KP) equations for right- and left-going waves, is found. KP models include versions of the KP-I and KP-II equations, in Cartesian and cylindrical geometry. Solitary waves solutions, planar or ring-shaped, and of dark or anti-dark type, are also predicted to occur. Their nature and stability is determined by a parameter defined by the physical parameters of the original nonlocal system. It is thus found that (dark) anti-dark solitary waves are only supported by a weak (strong) nonlocality, and are unstable (stable) in higher-dimensions. Our analytical predictions are corroborated by direct numerical simulations.

PACS numbers: 42.65.Tg, 05.45.Yv, 02.30.Mv

Submitted to: *J. Phys. A: Math. Gen.*

1. Introduction

In the theory of nonlinear waves, many problems appear where several different temporal and/or spatial scales are present. Thus, asymptotic multiscale expansion methods are usually applied to derive nonlinear evolution equations more manageable to the problem at hand [1]. By means of such asymptotic methods, it has been demonstrated that several systems integrable by the Inverse Scattering Transform (IST) [2] can be reduced to other integrable models [3]. Such connections have been proved extremely useful since solutions of the reduced models can be used to construct approximate solutions of the original models. A prominent example is the connection of the defocusing nonlinear Schrödinger (NLS) equation with the Korteweg-de Vries (KdV) equation, which allowed for the description of shallow dark solitons of the former in terms of KdV solitons. Relevant studies started in the early 70s [4] and continue to this date [5]; importantly, they have also been extended to the case of non-integrable systems, providing extremely

useful information on the existence, stability and dynamics of solutions in various physical settings, such as nonlinear optics [6] and Bose-Einstein condensates [7, 8].

Indeed, these methods become even more useful when the original system is not integrable without known solutions in explicit form. Models featuring a spatially nonlocal nonlinear response are important examples, since they are used to describe beam dynamics and solitons in various systems such as plasmas [9], atomic vapors [10], lead glasses featuring strong thermal nonlinearity [11], as well as media with a long-range inter-particle interaction. The latter include nematic liquid crystals with long-range molecular reorientational interactions [12], as well as dipolar bosonic quantum gases [13]. Importantly, nonlocality plays a key role on the soliton properties. In particular, in the case of focusing nonlocal nonlinearities, collapse does not take place in higher-dimensions [14, 15], which results in stable solitons, as observed in experiments of, say [10, 11], even in the $(3+1)$ -dimensional setting [16] – see, e.g., reviews [15, 17] and references therein. On the other hand, in the case of defocusing nonlocal nonlinearities, dark solitons that are supported in such settings [18–21], may exhibit an attractive interaction [18], rather than a repulsive one, as is the situation in the case of a local nonlinearity – cf. [6–8] and references therein. Furthermore, dark solitons which are known to be prone to the transverse (or “snaking”) instability in higher-dimensional settings [8, 22–24], can be stabilized due to the nonlocal nonlinearity [25].

Motivated by the above, and particularly by the fact that nonlocal nonlinearities have a profound effect on the form and stability properties of nonlinear excitations, in this work, we study a nonlocal defocusing NLS model in $(3+1)$ -dimensions. A brief description of our findings, as well as the outline of the presentation, is as follows.

First, in Section 2, we present the model which is considered in both physically relevant geometries: Cartesian and cylindrical. The model describes light beam propagation in nematic liquid crystals [26, 27] and thermal nonlinear media [15], and has been used to predict three-dimensional (3D) solitons [16, 17]. In addition, the continuous-wave (cw) solution is found and its stability is analysed. Then, in Section 3, we use multiscale expansion methods to derive asymptotic reductions of the nonlocal NLS equation. At an intermediate stage of the asymptotic analysis, we obtain a Boussinesq-type equation. Next, we consider the far-field of the Boussinesq equation, and derive various Kadomtsev-Petviashvili (KP) type models for right- and left-going waves. These models, which are classified in Section 4, include KP-I and KP-II equations, in Cartesian and cylindrical geometry (in the latter, the relevant model is also known as the Johnson equation [28]), as well as the Cylindrical-I (CI) and Cylindrical-II (CII) equations. All these models have been used to describe various physical situations ranging from shallow-water waves to ion-acoustic waves in plasmas, and so on [29–32]. In the same Section (Sec. 4), we present solitary waves of the original nonlocal model, which are constructed from solutions of the effective asymptotic equations. We thus find KdV-type, spatial dark or anti-dark solitary waves, namely intensity dips or humps on top of the cw-background, which may exhibit either a planar shape (stripes) or a cylindrical (ring) shape. Dark (anti-dark) solitary waves exist in a weak (strong) nonlocal regime, defined

by the sign of a characteristic quantity that links all the physical parameters of the original nonlocal system, and are unstable (stable) in the 2D setting. We also find temporal dark solitary waves which are predicted to be unstable in higher-dimensions. Our analytical predictions are found to be in very good agreement with results from direct numerical simulations: indeed, using the analytical forms of the spatial soliton solutions as initial conditions for the direct numerical integration of the original problem, we find that the solitons propagate undistorted – at least for relatively small propagation distances. Note that, even for longer propagation distances, instabilities are not observed in our simulations, which suggests that the solitons found have a good chance to be observed in experiments. Finally, in Section 5, we present our conclusions and highlight some interesting directions for future studies.

2. Model and continuous wave solution

We consider a $(3 + 1)$ -dimensional nonlocal NLS model, composed by a system of two coupled equations for the complex field amplitude u and the nonlinear correction to the refractive index n (which is a real function). This model applies, in particular, to light propagation in nematic liquid crystals [12, 26] and to thermal nonlinear optical media [15] (see also relevant theoretical and experimental work in [33]). The system under consideration is expressed in the following dimensionless form [16, 17]:

$$iu_z + \frac{1}{2}(\Delta u - Du_{tt}) - 2nu = 0, \quad (1)$$

$$d\Delta n - 2qn + 2|u|^2 = 0, \quad (2)$$

where subscripts denote partial derivatives, z is the propagation coordinate (normalized to the diffraction length), t is retarded time, and Δ is the transverse Laplacian. Below, we consider both physically relevant geometries, Cartesian and cylindrical, for which the Laplacian respectively reads:

$$\Delta = \partial_x^2 + \partial_y^2, \quad \Delta = \frac{1}{r}\partial_r(r\partial_r) + \frac{1}{r^2}\partial_\theta^2,$$

with transverse coordinates $\mathbf{r}_\perp = (x, y)$ or $\mathbf{r}_\perp = (r, \theta)$, respectively, normalized with respect to the beam width. Additionally, the real constants D , d , and q in Eqs. (1)-(2), which are assumed to be $\mathcal{O}(1)$ parameters in our analysis below, have the following physical significance. First, D represents the ratio of diffraction and dispersion lengths, with $D > 0$ ($D < 0$) corresponding to anomalous (normal) group-velocity dispersion (GVD). Second, in the context of nematic liquid crystals, the parameter q is related to the square of the applied static electric field that pre-tilts the nematic dielectric [27, 34, 35]. Third, parameter d measures the relative width of the response of the medium to the light field, and is connected to the nonlocality scale of the nonlinear response of the medium: in the limit $d \rightarrow 0$, the system of Eqs. (1)-(2) decouples and is reduced to a local $(3+1)$ -dimensional NLS equation with a cubic defocusing nonlinearity.

To start our analysis, we use the Madelung transformation

$$u = u_0\sqrt{\rho}\exp(i\phi), \quad (3)$$

(u_0 being an arbitrary complex constant) to separate the real functions for the amplitude ρ and phase ϕ of u in Eq. (1), and derive from Eqs. (1)-(2) the following system:

$$\phi_z + 2n + \frac{1}{2} (\nabla\phi)^2 - D\phi_t^2 - \frac{1}{2}\rho^{-1/2} \Delta\rho^{1/2} - D \rho^{1/2}{}_{tt} = 0, \quad (4)$$

$$\rho_z + \nabla \cdot (\rho\nabla\phi) - D(\rho\phi_t)_t = 0, \quad (5)$$

$$d\Delta n - 2qn + 2|u_0|^2\rho = 0, \quad (6)$$

where ∇ is the typical gradient vector operator, defined as:

$$\nabla = (\partial_x, \partial_y), \quad \nabla = \partial_r, \frac{1}{r}\partial_\theta$$

for the Cartesian or the cylindrical geometry, respectively.

It is readily observed that the above system possesses an exact steady-state solution of the form:

$$\phi = -\frac{2}{q}|u_0|^2 z, \quad \rho = 1, \quad n = \frac{1}{q}|u_0|^2,$$

which corresponds to the continuous-wave (cw) solution

$$u = u_0 \exp \left[-\frac{2i}{q}|u_0|^2 z \right], \quad n = \frac{1}{q}|u_0|^2, \quad (7)$$

of Eqs. (1)-(2). Note that the constant amplitude u_0 can be absorbed into ρ in the Madelung transformation; nevertheless, for convenience, we opt to use u_0 in Eq. (3) so that no extra free phase appears on the solutions that we present below, thus making presentation more clear. To further elaborate on this point, and also to underline the importance of this cw solution in our analysis (because the cw defines the background on top of which our solutions will propagate), let us write the solution of Eqs. (1)-(2) as

$$u = U_0(z)\bar{u}, \quad n = n_0\bar{n},$$

where the background (cw) solution satisfies

$$i\frac{dU_0}{dz} = 2n_0U_0, \quad n_0 = \frac{|U_0|}{q}.$$

Obviously, the solution of the above equations is given in Eq. (7), while \bar{u} and \bar{n} satisfy the system

$$i\bar{u}_z + \frac{1}{2}(\Delta\bar{u} - D\bar{u}_{tt}) - 2\frac{|u_0|^2}{q}(1 - \bar{n})\bar{u} = 0,$$

$$\frac{d}{q}\Delta\bar{n} - 2\bar{n} + 2|\bar{u}|^2 = 0.$$

This system possesses a cw solution of unit amplitude, as would be the case if u_0 was not used in the Madelung transformation (i.e., in other words, u_0 will inevitably appear in the cw background solution).

Below we seek nonlinear excitations (e.g., solitary waves) which propagate on top of this cw background. It is, thus, relevant to investigate if this solution is subject to modulational instability (MI): evidently, nonlinear excitations corresponding to an

unstable background do not have any physical purport. The stability of the cw solution can be investigated upon employing Eqs. (4)-(6) as follows. Let

$$\rho = 1 + \tilde{\rho}, \quad \phi = -\frac{2}{q}|u_0|^2 z + \tilde{\phi}, \quad n = \frac{1}{q}|u_0|^2 + \tilde{n},$$

where small perturbations $\tilde{\rho}$, $\tilde{\phi}$ and \tilde{n} are assumed to behave like $\exp[i(k_z z + \mathbf{k}_\perp \cdot \mathbf{r}_\perp - \omega t)]$. Here, we should recall that the evolution variable in our problem is the propagation distance z and, thus, the MI analysis is performed with respect to this variable; as such, k_z and its roots (real or imaginary) will determine the stability of the cw solution. To this end, substituting the above ansatz into Eqs. (4)-(6), we find that small-amplitude linear waves obey a dispersion relation of the following form,

$$k_z^2 = \frac{2|u_0|^2}{q}(\mathbf{k}_\perp^2 - D\omega^2) \left[1 + \frac{d\mathbf{k}_\perp^2}{2q} \right]^{-1} + \frac{1}{4}(\mathbf{k}_\perp^2 - D\omega^2)^2. \quad (8)$$

The results stemming from the above equation are as follows. First, Eq. (8) shows that the cw solution is always modulationally stable, i.e., $k_z \in \mathbb{R} \forall \mathbf{k}_\perp, \omega$, provided $D < 0$. Note, that in the (1+1)-dimensional case (corresponding to $k_y = 0$ and $D = 0$, or $\mathbf{k}_\perp = 0$ and $D = -1$), this result recovers the one of Ref. [15]. Second, if $D = |D| > 0$, the cw solution is unstable: in this case, perturbations grow exponentially, with the instability growth rate given by $\text{Im}(k_z)$. Thus, hereafter, we focus on this case, and assume that $D = -|D|$, corresponding to the anomalous GVD regime. It is, therefore, clear that the asymptotic analysis and results that we present in the following Sections are only valid in this regime; in the opposite case, of $D = |D| > 0$, since the cw background is unstable, any small perturbations on top of it will result in collapsing solutions.

Another physically relevant information stemming from Eq. (8) is that, in the long-wavelength and low-frequency limit (i.e., $|\mathbf{k}_\perp|, \omega \rightarrow 0$), small-amplitude spatial or temporal waves propagate on top of the cw background with “sound velocities” C^2 or V^2 , respectively, which are given by:

$$C^2 = \frac{2|u_0|^2}{q}, \quad V^2 = C^2|D|. \quad (9)$$

These characteristic velocities can also be determined, in a self-consistent manner, in the framework of the reductive perturbation method (see, e.g., Ref. [36]). It is also noted that in the unstable case of $D = |D| > 0$, velocity V becomes imaginary, a fact that also indicates that perturbations of the cw solution grow exponentially in the propagation distance z .

3. Effective nonlinear evolution equations

3.1. The Boussinesq equation

Observing that the dispersion relation (8) resembles the one of a Boussinesq equation [31, 32], we now derive from Eqs. (4)-(6) a Boussinesq equation, for either Cartesian or

cylindrical geometry. We thus seek solutions of Eqs. (4)-(6) in the form of the following asymptotic expansions:

$$\phi = -\frac{2}{q}|u_0|^2 z + \varepsilon^{1/2}\Phi, \quad \rho = 1 + \varepsilon\rho_1 + \varepsilon^2\rho_2 + \dots, \quad n = \frac{1}{q}|u_0|^2 + \varepsilon n_1 + \varepsilon^2 n_2 + \dots, \quad (10)$$

where ε is a formal small parameter ($0 < \varepsilon \ll 1$), while unknown real functions Φ , ρ_j and n_j are assumed to depend on “slow variables”. In particular, for the Cartesian geometry, Φ , ρ_j and n_j are taken to depend on $\{Z, X, Y, T\}$, while, for the cylindrical geometry, on $\{Z, R, \theta, T\}$ (the angular coordinate θ is assumed to remain unchanged); these slow variables are defined as:

$$Z = \varepsilon^{1/2}z, \quad X = \varepsilon^{1/2}x, \quad Y = \varepsilon^{1/2}y, \quad R = \varepsilon^{1/2}r, \quad T = \varepsilon^{1/2}t. \quad (11)$$

Substituting the expansions (10) into Eqs. (4)-(6), and using the variables in Eq. (11), we obtain the following results. First, Eq. (4) reads:

$$\Phi_Z + 2n_1 + \varepsilon \frac{1}{2} \mathbf{h} \cdot (\tilde{\nabla}\Phi)^2 + |D|\Phi_T^2 - \frac{1}{4} \tilde{\Delta}\rho_1 + |D|\rho_{1TT} + 2n_2 = \mathcal{O}(\varepsilon^2), \quad (12)$$

where

$$\tilde{\Delta} = \partial_X^2 + \partial_Y^2, \quad \tilde{\nabla} = (\partial_X, \partial_Y)$$

for the Cartesian case, while

$$\tilde{\Delta} = \frac{1}{R}\partial_R(R\partial_R) + \frac{1}{R^2}\partial_\theta^2, \quad \tilde{\nabla} = \partial_R, \frac{1}{R}\partial_\theta$$

for the cylindrical case. Second, Eq. (5) leads, at orders $\mathcal{O}(\varepsilon^{3/2})$ and $\mathcal{O}(\varepsilon^{5/2})$, to the following equations, respectively:

$$\rho_{1Z} + \tilde{\Delta}\Phi + |D|\Phi_{TT} = 0, \quad (13)$$

$$\rho_{2Z} + \tilde{\nabla} \cdot (\rho_1 \tilde{\nabla}\Phi) + |D|(\rho_1 \Phi_T)_T = 0. \quad (14)$$

Finally, Eq. (6), at orders $\mathcal{O}(\varepsilon)$ and $\mathcal{O}(\varepsilon^2)$, lead, respectively, to the equations:

$$-2qn_1 + 2|u_0|^2\rho_1 = 0, \quad (15)$$

$$d\tilde{\Delta}n_1 - 2qn_2 + 2|u_0|^2\rho_2 = 0. \quad (16)$$

The leading-order part of Eq. (12), together with Eq. (15), provides the following connection between functions Φ , n_1 and ρ_1 :

$$\Phi_Z = -2n_1 = -C^2\rho_1. \quad (17)$$

Furthermore, from the system of Eqs. (12)-(16), it is possible to eliminate functions $\rho_{1,2}$ and $n_{1,2}$, and derive the following equation for Φ :

$$\begin{aligned} \Phi_{ZZ} - C^2 \tilde{\Delta}\Phi + |D|\Phi_{TT} + \varepsilon \frac{1}{4C^2} \alpha \tilde{\Delta}\Phi + |D|\Phi_{TT} \quad \text{zz} \\ + \mathbf{h} \cdot (\tilde{\nabla}\Phi)^2 + |D|\Phi_T^2 + \Phi_Z \tilde{\Delta}\Phi + |D|\Phi_{TT} \quad \text{o} = \mathcal{O}(\varepsilon^2), \end{aligned} \quad (18)$$

where the parameter α is given by:

$$\alpha = 1 - \frac{4d|u_0|^2}{q^2}. \quad (19)$$

It is clear that, to leading-order, Eq. (18) is a linear wave equation indicating that the velocities of spatial or temporal waves are indeed those given in Eq. (9). In addition, at order $\mathcal{O}(\varepsilon)$, Eq. (18) incorporates fourth-order dispersion terms and quadratic nonlinear terms. Obviously, Eq. (18) is a Boussinesq-type equation, either in Cartesian or cylindrical coordinates, as per the discussion above. The Boussinesq equation has been originally proposed for studies of waves in shallow water [29, 31, 32], but later it was also used in different contexts, ranging from ion-acoustic waves in plasmas [29, 30] to mechanical lattices and electrical transmission lines [37].

A Boussinesq equation, similar to that in Eq. (18), was derived from a $(2 + 1)$ -dimensional NLS equation, in Cartesian coordinates, with a local defocusing nonlinearity [23]; earlier analysis of this Boussinesq model [38] was used in [23] to investigate self-focusing and transverse instability of plane dark solitons (see also [24] for a review and references therein). In fact, the Cartesian version of the Boussinesq model (18) is reduced to the one derived in [23] in the limit of $d \rightarrow 0$, i.e., in the local nonlinearity case.

3.2. Kadomtsev-Petviashvili-type equations

We now proceed to derive the far-field equations stemming from the Boussinesq model (18), in the framework of multiscale asymptotic expansions. As is known, the far-field of the Boussinesq equation in $(1 + 1)$ -dimensions is a pair of two KdV equations [32], while in $(2 + 1)$ -dimensions, it is a pair of KP equations [23], for right- and left-going waves. Below we show that Eq. (18) gives rise to $(3 + 1)$ -dimensional KP-type models for such waves. In addition, we will distinguish cases corresponding to two different types of solitary waves that may be supported either in Cartesian or cylindrical geometry: one, is oblique tube-shaped, oriented under a uniquely determined angle to the propagation axis, i.e., a *spatial solitary wave*; the other, is a constant-shape localized perturbation propagating along the z -axis, i.e., a *temporal solitary wave*.

3.2.1. Spatial solitary waves First, we consider spatial solitary waves, which may have either the form of stripes propagating on the XZ plane (Cartesian geometry), or exhibit an annular shape, with the ring radius varying with the propagation distance (cylindrical geometry). We thus introduce the variables:

$$\chi = X - CZ, \quad \tilde{\chi} = X + CZ, \quad \mathcal{Z} = \varepsilon Z, \quad \mathcal{Y} = \varepsilon^{1/2} Y, \quad \mathcal{T} = \varepsilon^{1/2} T,$$

and

$$\varrho = R - CZ, \quad \tilde{\varrho} = R + CZ, \quad \mathcal{Z} = \varepsilon Z, \quad \Theta = \varepsilon^{-1/2} \theta, \quad \mathcal{T} = \varepsilon^{1/2} T,$$

for the two geometries, respectively. We also look for solutions of Eq. (18) in the form of the asymptotic expansion:

$$\Phi = \Phi_0 + \varepsilon \Phi_1 + \dots \tag{20}$$

Substituting Eq. (20) into Eq. (18), we obtain the following results. At leading-order, $\mathcal{O}(1)$:

$$4C^2\Phi_{0\chi\tilde{\chi}} = 0, \quad 4C^2\Phi_{0\varrho\tilde{\varrho}} = 0, \quad (21)$$

for the Cartesian and cylindrical geometry, respectively. The above equations imply that, in each case, Φ_0 can be expressed as a superposition of a right-going wave, $\Phi_0^{(R)}$, depending on χ or ϱ , and a left-going one, $\Phi_0^{(L)}$, depending on $\tilde{\chi}$ or $\tilde{\varrho}$, namely:

$$\Phi_0 = \Phi_0^{(R)} + \Phi_0^{(L)}. \quad (22)$$

Second, at order $\mathcal{O}(\varepsilon)$:

$$\begin{aligned} 4C^2\Phi_{1\chi\tilde{\chi}} = & -C \left[\Phi_{0\chi\chi}^{(R)}\Phi_{0\tilde{\chi}}^{(L)} - \Phi_{0\chi}^{(R)}\Phi_{0\tilde{\chi}\tilde{\chi}}^{(L)} \right] \quad \# \\ & + \left[-2C\Phi_{0\mathcal{Z}}^{(R)} + \frac{\alpha}{4}\Phi_{0\chi\chi\chi}^{(R)} - \frac{3C}{2}\Phi_{0\chi}^{(R)2} \right]_{\chi} - C^2 \left[\Phi_{0\mathcal{Y}\mathcal{Y}}^{(R)} + |D|\Phi_{0\mathcal{T}\mathcal{T}}^{(R)} \right] \quad \# \\ & + \left[2C\Phi_{0\mathcal{Z}}^{(L)} + \frac{\alpha}{4}\Phi_{0\tilde{\chi}\tilde{\chi}\tilde{\chi}}^{(L)} + \frac{3C}{2}\Phi_{0\tilde{\chi}}^{(L)2} \right]_{\tilde{\chi}} - C^2 \left[\Phi_{0\mathcal{Y}\mathcal{Y}}^{(L)} + |D|\Phi_{0\mathcal{T}\mathcal{T}}^{(L)} \right], \quad (23) \end{aligned}$$

for the Cartesian geometry, and

$$\begin{aligned} 4C^2\Phi_{1\varrho\tilde{\varrho}} = & -C \left[\Phi_{0\varrho\varrho}^{(R)}\Phi_{0\tilde{\varrho}}^{(L)} - \Phi_{0\varrho}^{(R)}\Phi_{0\tilde{\varrho}\tilde{\varrho}}^{(L)} \right] \quad \# \\ & + \left[-2C\Phi_{0\mathcal{Z}}^{(R)} + \frac{\alpha}{4}\Phi_{0\varrho\varrho\varrho}^{(R)} - \frac{3C}{2}\Phi_{0\varrho}^{(R)2} - \frac{C}{\mathcal{Z}}\Phi_0^{(R)} \right]_{\varrho} - \frac{1}{\mathcal{Z}^2}\Phi_{0\theta\theta}^{(R)} - V^2\Phi_{0\mathcal{T}\mathcal{T}}^{(R)} \quad \# \\ & + \left[2C\Phi_{0\mathcal{Z}}^{(L)} + \frac{\alpha}{4}\Phi_{0\tilde{\varrho}\tilde{\varrho}\tilde{\varrho}}^{(L)} + \frac{3C}{2}\Phi_{0\tilde{\varrho}}^{(L)2} - \frac{C}{\mathcal{Z}}\Phi_0^{(L)} \right]_{\tilde{\varrho}} - \frac{1}{\mathcal{Z}^2}\Phi_{0\theta\theta}^{(L)} - V^2\Phi_{0\mathcal{T}\mathcal{T}}^{(L)}. \quad (24) \end{aligned}$$

for the cylindrical geometry. Upon integrating Eq. (23) in χ or $\tilde{\chi}$ [Eq. (24) in ϱ or $\tilde{\varrho}$], it is obvious that the terms in square brackets in the right-hand side are secular, because are functions of χ or $\tilde{\chi}$ (of ϱ or $\tilde{\varrho}$) alone. Removal of these terms leads to two uncoupled nonlinear evolution equations for $\Phi_0^{(R)}$ and $\Phi_0^{(L)}$. Furthermore, employing Eq. (17), it is straightforward to find that the amplitude ρ_1 can also be decomposed to a left- and a right-going wave, i.e., $\rho_1 = \rho_1^{(R)} + \rho_1^{(L)}$, with

$$\Phi_{0\chi}^{(R)} = C\rho_1^{(R)}, \quad \Phi_{0\tilde{\chi}}^{(L)} = -C\rho_1^{(L)}, \quad \text{and} \quad \Phi_{0\varrho}^{(R)} = C\rho_1^{(R)}, \quad \Phi_{0\tilde{\varrho}}^{(L)} = -C\rho_1^{(L)}.$$

Then, using the above expressions, the equations for $\Phi_0^{(R)}$ and $\Phi_0^{(L)}$ yield, in each geometry, two uncoupled equations for $\rho_1^{(R)}$ and $\rho_1^{(L)}$. In Cartesian geometry, these equations are:

$$\rho_{1\mathcal{Z}}^{(R)} - \frac{\alpha}{8C}\rho_{1\chi\chi\chi}^{(R)} + \frac{3C}{2}\rho_1^{(R)}\rho_{1\chi}^{(R)} \quad \chi + \frac{C}{2} \left[\rho_{1\mathcal{Y}\mathcal{Y}}^{(R)} + |D|\rho_{1\mathcal{T}\mathcal{T}}^{(R)} \right] = 0, \quad (25)$$

$$\rho_{1\mathcal{Z}}^{(L)} + \frac{\alpha}{8C}\rho_{1\tilde{\chi}\tilde{\chi}\tilde{\chi}}^{(L)} - \frac{3C}{2}\rho_1^{(L)}\rho_{1\tilde{\chi}}^{(L)} \quad \tilde{\chi} - \frac{C}{2} \left[\rho_{1\mathcal{Y}\mathcal{Y}}^{(L)} + |D|\rho_{1\mathcal{T}\mathcal{T}}^{(L)} \right] = 0. \quad (26)$$

On the other hand, equations for $\rho_1^{(R,L)}$ in cylindrical geometry, are:

$$\rho_{1\mathcal{Z}}^{(R)} - \frac{\alpha}{8C}\rho_{1\varrho\varrho\varrho}^{(R)} + \frac{3C}{2}\rho_1^{(R)}\rho_{1\varrho}^{(R)} + \frac{1}{2\mathcal{Z}}\rho_1^{(R)} \quad \varrho + \frac{1}{2C} \left[\frac{1}{\mathcal{Z}^2}\rho_{1\theta\theta}^{(R)} + V^2\rho_{1\mathcal{T}\mathcal{T}}^{(R)} \right] = 0, \quad (27)$$

$$\rho_{1\mathcal{Z}}^{(L)} + \frac{\alpha}{8C}\rho_{1\tilde{z}\tilde{z}\tilde{z}}^{(L)} - \frac{3C}{2}\rho_{1\tilde{z}}^{(L)}\rho_{1\tilde{z}}^{(L)} - \frac{1}{2\mathcal{Z}}\rho_{1\tilde{z}}^{(L)} - \frac{1}{2C}\frac{1}{\mathcal{Z}^2}\rho_{1\theta\theta}^{(L)} + V^2\rho_{1\tau\tau}^{(L)} = 0. \quad (28)$$

3.2.2. Temporal solitary waves We now proceed with the case of temporal solitary waves. First, introduce the variables:

$$\tau = T - VZ, \quad \tilde{\tau} = T + VZ, \quad \mathcal{Z} = \varepsilon Z,$$

as well as

$$\mathcal{X} = \varepsilon^{1/2}X, \quad \mathcal{Y} = \varepsilon^{1/2}Y, \quad \text{and} \quad \mathcal{R} = \varepsilon^{1/2}R, \quad \Theta = \varepsilon^{-1/2}\theta,$$

for the Cartesian and cylindrical geometry, respectively. Then, in each case, utilizing the above variables and the asymptotic expansion (20), we obtain from Eq. (18) the leading-order equation:

$$4V^2\Phi_{0\tau\tilde{\tau}} = 0,$$

which yields again Eq. (22). Furthermore, working as in the previous case, we obtain at order $\mathcal{O}(\varepsilon)$:

$$\begin{aligned} 4V^2\Phi_{1\tau\tilde{\tau}} &= -V|D| \left[\Phi_{0\tau\tau}^{(R)}\Phi_{0\tilde{\tau}}^{(L)} - \Phi_{0\tau}^{(R)}\Phi_{0\tilde{\tau}\tilde{\tau}}^{(L)} \right. \\ &+ \left. -2V\Phi_{0\mathcal{Z}}^{(R)} + \frac{D^2}{4}\Phi_{0\tau\tau\tau}^{(R)} - \frac{3|D|V}{2}\Phi_{0\tau}^{(R)2} \right]_{\tau} - C^2\hat{\Delta}\Phi_0^{(R)}, \\ &+ \left. 2V\Phi_{0\mathcal{Z}}^{(L)} + \frac{D^2}{4}\Phi_{0\tilde{\tau}\tilde{\tau}\tilde{\tau}}^{(L)} + \frac{3|D|V}{2}\Phi_{0\tilde{\tau}}^{(L)2} \right]_{\tilde{\tau}} - C^2\hat{\Delta}\Phi_0^{(L)}, \end{aligned} \quad (29)$$

where

$$\hat{\Delta} = \partial_{\mathcal{X}}^2 + \partial_{\mathcal{Y}}^2, \quad \hat{\Delta} = \frac{1}{\mathcal{R}}\partial_{\mathcal{R}}(\mathcal{R}\partial_{\mathcal{R}}) + \frac{1}{\mathcal{R}^2}\partial_{\Theta}^2,$$

for the two geometries, respectively. Then, employing Eq. (17), the amplitude ρ_1 is again expressed as $\rho_1 = \rho_1^{(R)} + \rho_1^{(L)}$, with

$$\Phi_{0\tau}^{(R)} = \frac{C^2}{V}\rho_1^{(R)}, \quad \Phi_{0\tilde{\tau}}^{(L)} = -\frac{C^2}{V}\rho_1^{(L)}. \quad (30)$$

Using Eqs. (30), we obtain from Eq. (29) the following equations for $\rho_1^{(R,L)}$:

$$\rho_{1\mathcal{Z}}^{(R)} - \frac{D^2}{8V}\rho_{1\tau\tau\tau}^{(R)} + \frac{3V}{2}\rho_{1\tau}^{(R)}\rho_{1\tau}^{(R)} + \frac{V}{2|D|}\hat{\Delta}\rho_1^{(R)} = 0, \quad (31)$$

$$\rho_{1\mathcal{Z}}^{(L)} + \frac{D^2}{8V}\rho_{1\tilde{\tau}\tilde{\tau}\tilde{\tau}}^{(L)} - \frac{3V}{2}\rho_{1\tilde{\tau}}^{(L)}\rho_{1\tilde{\tau}}^{(L)} - \frac{V}{2|D|}\hat{\Delta}\rho_1^{(L)} = 0. \quad (32)$$

We conclude this section with the observation that all equations that were derived for $\rho_1^{(R,L)}$ are of the KP type, in both geometries. Below we elaborate more on these effective models, and focus on limiting cases corresponding to their lower-dimensional versions. For simplicity, we only consider the right-going waves, $\rho_1^{(R)}$, since $\rho_1^{(L)}(\mathcal{Z}) = \rho_1^{(R)}(-\mathcal{Z})$. In addition, we will present examples of solitary wave solutions of Eqs. (1)-(2) arising from these KP models.

4. Versions of the KP equations and solitary waves

4.1. Classification of the effective KP models

First of all, it is convenient to further normalize the effective KP equations derived in the previous section in order to express them in their “standard” form [2, 30].

Consider, first, equations for spatial solitary waves, and introduce the transformations:

$$\mathcal{Z} \rightarrow -\frac{\alpha}{8C}\mathcal{Z}, \quad \mathcal{T} \rightarrow \frac{\sqrt{3|\alpha|}}{4V^2}\mathcal{T}, \quad (33)$$

as well as

$$\mathcal{Y} \rightarrow \frac{\sqrt{3|\alpha|}}{4C^2}\mathcal{Y}, \quad \rho_1^{(R)} = -\frac{\alpha}{2C^2}U \quad \text{and} \quad \Theta \rightarrow \frac{\sqrt{3|\alpha|}}{4}\Theta, \quad \rho_1^{(R)} = -\frac{\alpha}{2C^2}W,$$

for the Cartesian and cylindrical geometry, respectively. This way, Eq. (25) is expressed as:

$$(U_{\mathcal{Z}} + 6UU_{\mathcal{X}} + U_{\mathcal{X}\mathcal{X}\mathcal{X}})_{\mathcal{X}} + 3\sigma^2(U_{\mathcal{Y}\mathcal{Y}} + U_{\mathcal{T}\mathcal{T}}) = 0, \quad (34)$$

while Eq. (27) reads:

$$W_{\mathcal{Z}} + 6WW_{\mathcal{e}} + W_{\mathcal{e}\mathcal{e}\mathcal{e}} + \frac{1}{2\mathcal{Z}}W_{\mathcal{e}} + 3\sigma^2 \frac{1}{\mathcal{Z}^2}W_{\Theta\Theta} + W_{\mathcal{T}\mathcal{T}} = 0. \quad (35)$$

In the above equations, parameter σ^2 is given by

$$\sigma^2 = -\text{sgn}\alpha,$$

and it is reminded that α is given by Eq. (19).

The (1+1)-dimensional versions of Eqs. (34) and (35), i.e., the ones referring to the $\mathcal{Z}\mathcal{X}$ and $\mathcal{Z}\mathcal{e}$ plane, have respectively the form of a KdV and a cylindrical KdV (cKdV) equation. Both models are completely integrable by means of the IST [2], and find numerous applications in a variety of physical contexts [30–32, 37]. The KdV and cKdV equations have been derived by means of multiscale expansion methods from local NLS models, with the aim to describe shallow planar dark solitons in Bose gases [4] and ring dark solitons in nonlinear optical media [39] (see also reviews [6, 7] and references therein). More recently, a KdV equation was derived from the (1+1)-dimensional version of Eqs. (1)-(2) for $D = 0$, and used to describe small-amplitude nematicons [21]; in fact, the KdV model derived in [21] is identical with the (1+1)-dimensional version of Eq. (25) [or (34)].

Furthermore, there are two distinct (2+1)-dimensional versions of Eq. (34): a spatial one, in the $\mathcal{Z}\mathcal{X}\mathcal{Y}$ space, and a spatio-temporal one, in the $\mathcal{Z}\mathcal{X}\mathcal{T}$ space. These effective models can be used to describe either spatial optical solitons in nematic liquid crystals [26], or dispersion-induced dynamics of spatial solitons in thermal media [15]. Both these (2+1)-dimensional equations, are completely integrable by means of the IST [2].

Importantly, the (2+1)-dimensional versions, as well as the complete Eq. (34), include both versions of the KP equation, KP-I and KP-II [2]. Indeed, for $\sigma = 1$, i.e.,

$\alpha < 0 \Rightarrow d > (q/2|u_0|)^2$, Eq. (34) is a KP-II equation; on the other hand, for $\sigma = i$, i.e., $\alpha > 0 \Rightarrow d < (q/2|u_0|)^2$, Eq. (34) is a KP-I equation. Recalling that d is the degree of nonlocality of the system at hand (for $d \rightarrow 0$ nonlocal NLS Eqs. (1)-(2) become local), it is evident that relatively weak (strong) nonlocality, as defined by the above regimes of d , corresponds to a KP-I (KP-II) model. This fact has also important implications on the type and the stability of low-dimensional solitary waves that can be supported in the system (see below).

Similarly, we observe that there are two distinct $(2 + 1)$ -dimensional versions of Eq. (35): a spatial one, in the $\mathcal{Z}\varrho\Theta$ space, and a spatio-temporal one, in the $\mathcal{Z}\varrho\mathcal{T}$ space, which find applications in the contexts discussed above in the Cartesian case. The spatial version of Eq. (35) is a cylindrical KP (cKP) equation, which is also known as the Johnson's equation [28], and describes nearly-concentric solitons in an ideal, inviscid fluid [31]. This model is, also, completely integrable by means of the IST [40]. On the other hand, in the $\mathcal{Z}\varrho\mathcal{T}$ space, Eq. (27) reduces to the so-called CI equation, which describes weak cylindrical ion-acoustic solitons in plasmas [30]. Unlike the Johnson's equation, the CI equation is not considered to be integrable, as it fails to pass the Painlevé test [2].

It is interesting to point out that there exist transformations mapping solutions of the KP and cKP equations [31]. Indeed, the map:

$$U(\mathcal{Z}, \chi, \mathcal{Y}) \rightarrow W(\mathcal{Z}, \varrho, \Theta) := U \left(\mathcal{Z}, \varrho - \frac{\mathcal{Z}\Theta^2}{12\sigma^2}, \mathcal{Z}\Theta \right),$$

transforms any solution of the KP equation (34) into a solution of the cKP equation (35); conversely, the map:

$$W(\mathcal{Z}, \chi, \Theta) \rightarrow U(\mathcal{Z}, \chi, \mathcal{Y}) := W \left(\mathcal{Z}, \chi + \frac{\mathcal{Y}^2}{12\sigma^2\mathcal{Z}}, \frac{\mathcal{Y}}{\mathcal{Z}} \right),$$

transforms any solution of the cKP equation (35) into a solution of the KP equation (34). Here, we should also note that the spatial $(2 + 1)$ -dimensional versions of KP Eq. (34) and cKP Eq. (35) are also connected with another relevant model, the elliptic cKP (ecKP), that was recently presented and studied in [41]. In this work, it was shown that the ecKP model describes surface gravity waves of nearly elliptic fronts, and it is completely integrable. Based on the similarities of the hydrodynamic form (4)-(6) of the nonlocal NLS Eqs. (1)-(2) to the problem formulation of [41], we conjecture that, adopting an elliptic cylindrical coordinate system and following the lines of the analysis presented here, one could derive a $(3 + 1)$ -dimensional version of the ecKP equation. Nevertheless, such a derivation is beyond the scope of the present work.

We now turn our attention to the KP models that describe temporal waves. As before, first we put Eqs. (31) in the "standard" form. We thus introduce the transformations:

$$\mathcal{Z} \rightarrow -\frac{D^2}{8V}\mathcal{Z}, \quad \{\mathcal{X}, \mathcal{Y}, \mathcal{R}\} \rightarrow \sqrt{\frac{3|D|^3}{4V^2}}\{\mathcal{X}, \mathcal{Y}, \mathcal{R}\}, \quad \rho_1^{(R)} = -\frac{D^2}{2V^2}Q, \quad (36)$$

and obtain from Eqs. (31) the models:

$$(Q_{\mathcal{Z}} + 6QQ_{\tau} + Q_{\tau\tau\tau})_{\tau} - 3\hat{\Delta}Q = 0, \quad (37)$$

and it is reminded that the Laplacian $\hat{\Delta}$ refers to either the Cartesian or the cylindrical geometry. Obviously, the $(1+1)$ -dimensional version of Eq. (37) is the KdV equation. On the other hand, it is observed that, unlike the case of spatial solitary waves, the Cartesian version of Eq. (37) is solely of the KP-I type; in fact, in this case, transverse effects are not governed by the sign of parameter α . The $(2+1)$ -dimensional version of Eq. (37) is completely integrable by means of the IST [2]. Finally, the cylindrical version of Eq. (37) is known as the CII equation, and describes cylindrical ion-acoustic solitons in plasmas [30].

4.2. Solitary wave solutions

The asymptotic reduction of the nonlocal NLS equations to the effective equations above, allows for the derivation of approximate solutions of Eqs. (1)-(2), valid up to – and including – order $\mathcal{O}(\varepsilon)$. Of particular interest are solitary wave solutions, which can be constructed from solutions of Eqs. (34), (35) and (37). These asymptotic reductions provide information on the type of the solitary wave, as well as on the stability of lower-dimensional solutions in higher-dimensional settings. Below, we showcase some characteristic examples along those lines.

Let us first consider the case of spatial solitary waves. The $(1+1)$ -dimensional version of Eq. (34) is a KdV equation which possesses the commonly known soliton solution:

$$U = 2\kappa^2 \text{sech}^2[\kappa(\chi - 4\kappa^2\mathcal{Z} - \chi_0)], \quad (38)$$

where κ and χ_0 are constants. Using this solution, and reverting transformations for the independent variables and fields, we find the following approximate solution to Eqs. (1)-(2):

$$u \approx u_0 \left[1 - \frac{\varepsilon\kappa^2}{C^2} \alpha \text{sech}^2(\xi) \right] \exp \left[-\frac{2i}{q} |u_0|^2 z - i \frac{\varepsilon^{1/2}\kappa}{C} \alpha \tanh(\xi) \right], \quad (39)$$

$$n \approx \frac{1}{q} + \frac{1}{2} \varepsilon \kappa^2 \alpha \text{sech}^2(\xi), \quad (40)$$

$$\xi \equiv \varepsilon^{1/2} \kappa (x - v_s z - x_0), \quad v_s \equiv C \left[1 - \frac{1}{2} \frac{\varepsilon \eta^2}{C^2} |\alpha| \right]. \quad (41)$$

The solution for u has the form of either a density dip (for $\alpha > 0$) or a density hump (for $\alpha < 0$) on top of the cw background, with a tanh-shaped phase jump across the density minimum or maximum, respectively. It is thus either a dark soliton (for $\alpha > 0$) or an anti-dark soliton (for $\alpha < 0$); note that the soliton velocity v_s is slightly below the speed of sound, as is the case of shallow dark solitons in local media [6, 7]. Note that if $d \rightarrow 0$, then $\alpha > 0$, which means that in the case of the local system the soliton is always dark. In other words, anti-dark solitons are only supported due to the presence of nonlocality, in accordance with the analysis of [21].

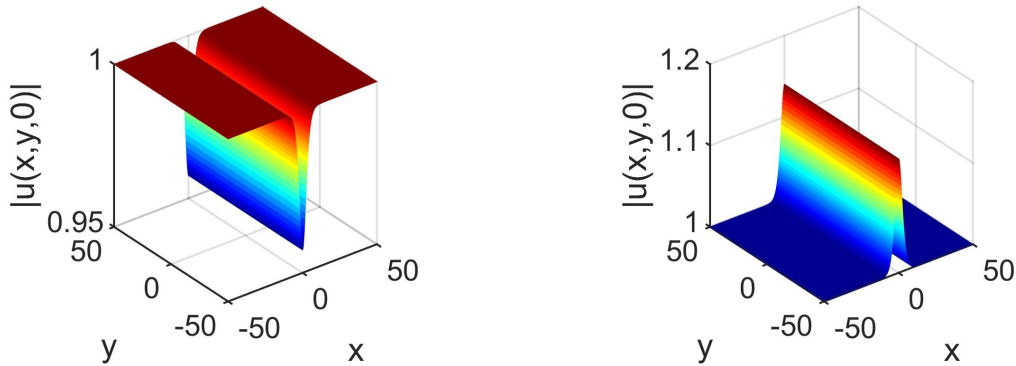


Figure 1. (Color Online) Typical dark (left) and anti-dark soliton (right) profiles, at $z = 0$, in Cartesian geometry, for $q = 1$ and $q = 5$, respectively. All other parameter values are equal to unity.

In Fig. 1, we depict the soliton solutions in Cartesian geometry according to Eq. (38). Here, solutions' profiles are plotted at $z = 0$; all parameter values are kept equal to unity, and we vary parameter q so that to obtain a dark and an anti-dark soliton, for $q = 1$ and $q = 5$, respectively. Furthermore, we use these profiles as initial conditions, and perform a direct numerical integration of Eqs. (1)-(2) to determine their evolution. For the simulations, we used a high accuracy spectral integrator in Cartesian coordinates. The results are shown in the contour plots of Fig. 2, where it is verified that these solutions maintain their stability – at least for relatively short propagation distances (see discussion below) – and propagating characteristics. Notice that, as expected from the analysis, the anti-dark soliton propagates at higher, though constant, velocity from its dark soliton counterpart.

The fact that Eq. (34) is either a KP-I (for $\alpha < 0$) or a KP-II (for $\alpha > 0$) equation, can be used to deduce stability of the approximate solitons in (2+1)-dimensions. Indeed, as is well known [2], line soliton solutions of KP-I are unstable, while those of KP-II are stable. This leads to the prediction that, in the context of the original problem, dark soliton stripes of the nonlocal problem will be unstable in the 2D setting, while anti-dark soliton stripes will be stable. Note that the instability in the context of the KP-I model was analyzed [38] and connected to the context of self-focusing and transverse instability of plane dark solitons in media with local defocusing nonlinearity [22, 23] (see also [24] for a review and references therein). It should also be mentioned that in the case of KP-I (for $\alpha < 0$), there exist “lump” solitons which are stable in the 2D setting [2]; these structures can be used to construct approximate solutions of the original problem which, in our case, will be 2D dark solitary waves, featuring an algebraic decay. These “lump” solitons, however (along with the planar ones discussed above), are unstable in the full (3 + 1)-dimensional setting [42].

We now turn to the case of the cylindrical geometry, and consider the (1 + 1)-dimensional version of Eq. (35), namely the cKdV equation. As mentioned above, this model is completely integrable by means of the IST. The solitary wave solution, which is

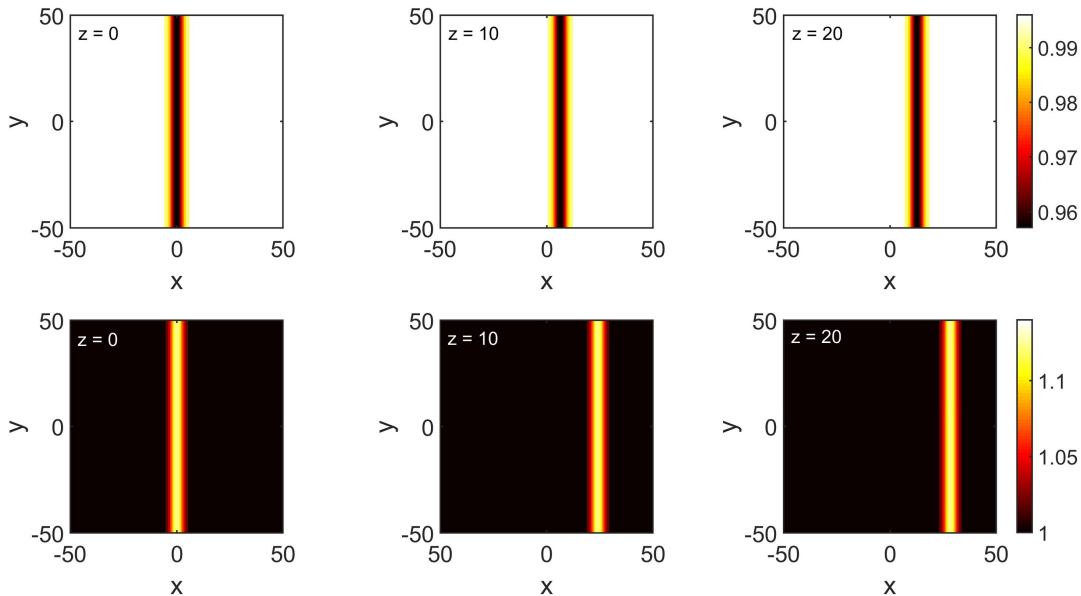


Figure 2. (Color Online) Contour plots showing the evolution of the dark (top) and anti-dark (bottom) solitons of Fig. 1. Results have been obtained from direct numerical integration of Eqs. (1)-(2).

expressed in terms of the Airy function [43], is composed of a primary wave and a shelf. An asymptotic analysis [44, 45] in the regime $|\mathcal{Z}| \gg |\varrho|$ shows the following: to leading-order approximation, the primary wave $W(\varrho, \mathcal{Z})$, that decays to zero at both upstream and downstream infinity, has a form similar to that of Eq. (38), with the obvious changes $\chi \rightarrow \varrho$ and $\chi_0 \rightarrow \varrho_0$, but with an important difference: κ now becomes a slowly-varying function of \mathcal{Z} , due to the presence of the term $W/(2\mathcal{Z})$. In fact, according to the analysis of Refs. [44, 45], and using the original coordinates, the following result can be obtained,

$$\kappa^2 = \kappa_0^2 \frac{z_0}{z}{}^{2/3}, \quad (42)$$

where κ_0^2 is a constant setting the solitary wave amplitude at $z = z_0$. Then, it is straightforward to express an approximate solution of Eqs. (1)-(2), but now for the cylindrical geometry, and for the primary solitary wave. This is of the form of Eqs. (39)-(41), but with the solitary wave amplitude and velocity varying as $z^{-2/3}$, and the width varying as $z^{1/3}$, as follows from Eqs. (38) and (42).

Obviously, this approximate solution is a ring-shaped solitary wave, on top of the cw background, which is either of the dark type (for $\alpha > 0$) or of the anti-dark type (for $\alpha < 0$). Note that ring dark solitons were predicted to occur in optical media exhibiting either Kerr [39] or non-Kerr [36] nonlinearities, and were later observed in experiments [46]. On the other hand, ring anti-dark solitons were only predicted to occur in non-Kerr – e.g., saturable media [36, 47]. This picture is complemented by our analysis, according to which a relatively strong [i.e., $d > (q/2|u_0|)^2$] nonlocal nonlinearity can also support ring anti-dark solitary waves.

In Fig. 3, typical ring dark and anti-dark soliton profiles, with parameter values

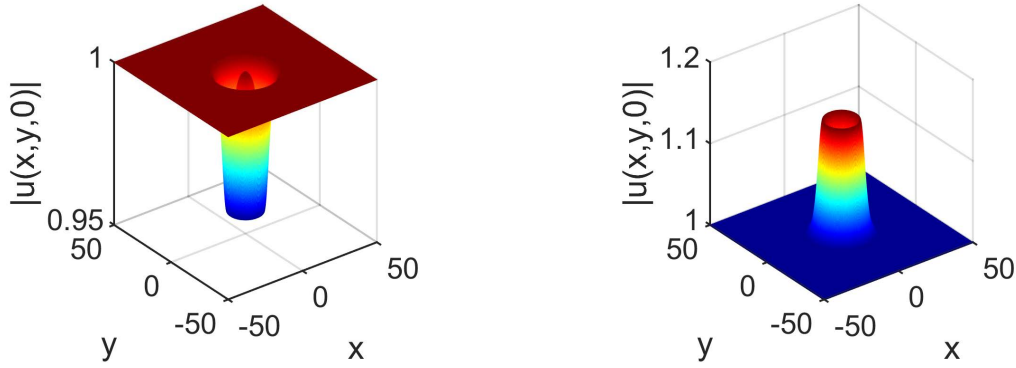


Figure 3. (Color Online) Typical ring dark (left) and anti-dark soliton profiles, at $z = 0$. Both solitons have an initial radius $r_0 = 10$, while other parameter values are as in the Cartesian case.

identical to those used in the Cartesian case, are shown at $z = 0$; both solitons have an initial radius of $r_0 = 10$. In addition, in Fig. 4, contour plots depicting the evolution of the solitons' densities are shown; these results, as before, have been obtained via direct numerical integration of Eqs. (1)-(2). Much like the Cartesian case, the solitons propagate undistorted, i.e., the initial rings expand outwards, keeping their shapes during the evolution – at least for relatively short propagation distances (see below). It is also observed that the solitons expand (propagate) with constant speed, with the anti-dark soliton expanding faster than the dark one: indeed, the anti-dark soliton's radius is larger than that of the dark one, at the same propagation distance.

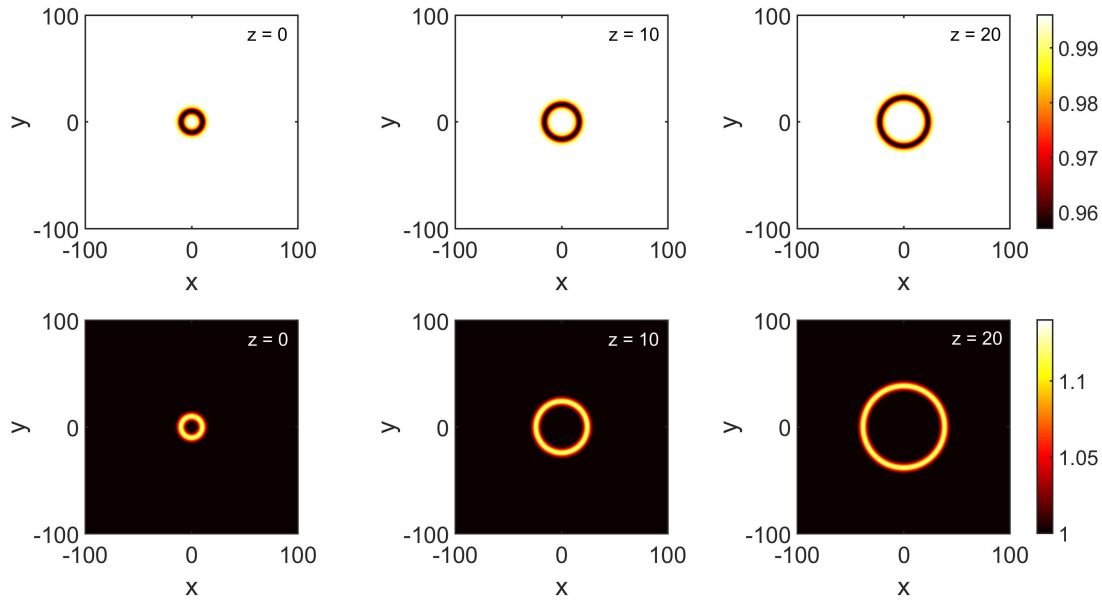


Figure 4. (Color Online) Contour plots showing the evolution of the ring dark (top) and anti-dark (bottom) ring solitons of Fig. 3. Results have been obtained from direct numerical integration of Eqs. (1)-(2).

As in the Cartesian case, the effective equation (35) can also be used to predict (in)stability of the ring dark or anti-dark solitary waves in the $(2 + 1)$ -dimensional setting. In particular, and similarly to the case of the planar solitons of Eq. (34), the case of $\alpha < 0$ ($\alpha > 0$), where ring dark (anti-dark) solitary waves exist, corresponds to a KP-I (KP-II) type model. It is, thus, clear that ring dark solitary waves are expected to be unstable, while ring anti-dark ones are predicted to be stable.

Finally, let us briefly discuss the case of temporal solitary waves described by Eq. (37). In the $(1 + 1)$ -dimensional setting, the underlying KdV equation has a soliton solution similar to that in Eq. (38), with the obvious changes $\chi \rightarrow \tau$ and $\chi_0 \rightarrow \tau_0$. However, when expressed in terms of the original fields and variables of Eqs. (1)-(2), it is clear that the corresponding approximate solitary wave solution is solely of the dark type: this is due to the fact that parameter α is not involved in the normalization of the field Q [cf. Eq. (36)]. For the same reason, as was also mentioned in the previous section, the higher-dimensional versions of Eq. (37) are solely of the KP-I type. As a result, in the Cartesian $(2 + 1)$ -dimensional setting corresponding to the usual KP-I model, one expects the existence of stable dark “lump” solitary wave solutions of the original model; these, however, are unstable in the full 3D setting [42]. Finally, regarding the cylindrical geometry, to the best of our knowledge, two-dimensional soliton solutions of the CII model are not known.

5. Conclusion

In conclusion, using multiscale expansion methods, we derived asymptotic reductions of $(3 + 1)$ -dimensional nonlocal NLS equations, that are used to describe nonlinear waves in nematic liquid crystals and media with a thermal nonlinearity. Working on the hydrodynamic form of the model, both in Cartesian and cylindrical geometries, first we derived, at an intermediate stage of the asymptotic analysis, a 3D Boussinesq equation. Then, we considered two cases, corresponding to spatial or temporal structures and, upon introducing relevant scales and asymptotic expansions, we reduced the Boussinesq model to KP-type equations that govern right- and left-propagating waves. These models include various integrable and non-integrable equations at different dimensionalities and geometries, such as the KdV and the cKdV equation, the KP-I and KP-II equations, Johnson’s equation, as well as the CI and CII equations.

We also employed these models to construct approximate solitary wave solutions of the original nonlocal NLS model. Note that a complete discussion of the various solutions and their properties will be provided in a later communication. As such, useful results were deduced on the type and the stability of lower-dimensional solitary waves in higher-dimensional settings. In that regard, we identified parameter regimes, corresponding to relatively weak or strong nonlocality, for which we predicted the existence and stability of various solitary waves. Thus, we predicted the existence of spatial, planar or cylindrical (ring-shaped), dark or anti-dark solitary waves, for weak or strong nonlocality, respectively, and that dark (anti-dark) solitary waves are

unstable (stable) in the $(2+1)$ -dimensional setting. Furthermore, our analysis suggested the existence of temporal solitary waves, which become unstable in higher dimensions. Regarding approximate two-dimensional solitary wave solutions, it was found that they may exist in the form of algebraically decaying dark “lumps”, which satisfy effective KP-I models; such structures may be either of the spatial or temporal type and are supported in the weak nonlocality regime.

Our analytical predictions were also corroborated by results of direct numerical simulations. Indeed, we have used the analytical forms of the spatial soliton profiles, in both the Cartesian and the cylindrical geometry, we have studied their evolution stemming from the direct numerical integration of the original nonlocal model. We have thus found that both the dark and anti-dark soliton stripes and rings propagate undistorted, as per the effective KP picture, at least for short propagation distances. Notice that, even for longer propagation distances, instabilities were not observed in our simulations, which suggests that the solitons presented here have a good chance to be observed in experiments.

Our analysis suggests various interesting directions for future studies. For instance, it would be relevant to extend our considerations to nonlocal models with a higher number of components (see, e.g., [48]). In that case, it would be important to identify vector solitary waves in these models, such as dark-dark and dark-bright, extending previous studies in media with a defocusing local nonlinearity [8].

References

- [1] A. Jeffrey and T. Kawahara. *Asymptotic methods in nonlinear wave theory*. Pitman, 1982.
- [2] M. J. Ablowitz and P. A. Clarkson. *Solitons, nonlinear evolution equations and inverse scattering*. Cambridge University Press, 1991.
- [3] V. E. Zakharov and E. A. Kuznetsov. Multi-scale expansions in the theory of systems integrable by the inverse scattering transform. *Physica D*, 18:455–463, 1986.
- [4] T. Tsuzuki. Nonlinear waves in the Pitaevskii-Gross equation. *J. Low Temp. Phys.*, 4:441–457, 1971.
- [5] T. P. Horikis and D. J. Frantzeskakis. On the NLS to KdV connection. *Rom. J. Phys.*, 59:195–203, 2014.
- [6] Yu. S. Kivshar and B. Luther-Davies. Dark optical solitons: physics and applications. *Phys. Rep.*, 298:81–197, 1998.
- [7] D. J. Frantzeskakis. Dark solitons in Bose-Einstein condensates: from theory to experiments. *J. Phys. A: Math. Theor.*, 43:213001, 2010.
- [8] P. G. Kevrekidis, D. J. Frantzeskakis, and R. Carretero-González. *The defocusing nonlinear Schrödinger equation: from dark solitons to vortices and vortex rings*. SIAM, 2015.
- [9] A. G. Litvak, V. A. Mironov, G. M. Fraiman, and A. D. Yunakovskii. Thermal self-effect of wave beams in a plasma with a nonlocal nonlinearity. *Sov. J. Plasma Phys.*, 1:60–71, 1975.
- [10] D. Suter and T. Blasberg. Stabilization of transverse solitary waves by a nonlocal response of the nonlinear medium. *Phys. Rev. A*, 48:4583–4587, 1993.
- [11] C. Rotschild, T. Carmon, O. Cohen, O. Manela, and M. Segev. Solitons in nonlinear media with an infinite range of nonlocality: first observation of coherent elliptic solitons and of vortex-ring solitons. *Phys. Rev. Lett.*, 95:213904, 2005.

- [12] C. Conti, M. Peccianti, and G. Assanto. Route to nonlocality and observation of accessible solitons. *Phys. Rev. Lett.*, 91:073901, 2003.
- [13] P. Pedri and L. Santos. Two-dimensional bright solitons in dipolar Bose-Einstein condensates. *Phys. Rev. Lett.*, 95:200404, 2005.
- [14] S. K. Turitsyn. Spatial dispersion of nonlinearity and stability of many dimensional solitons. *Theor. Math. Phys.*, 64:797–801, 1985.
- [15] W. Krolikowski, O. Bang, N. I. Nikolov, D. Neshev, J. Wyller, J. J. Rasmussen, and D. Edmundson. Modulational instability, solitons and beam propagation in spatially nonlocal nonlinear media. *J. Opt. B: Quantum Semiclass. Opt.*, 6:S288–S294, 2004.
- [16] D. Mihalache, D. Mazilu, F. Lederer, B. A. Malomed, Y. V. Kartashov, L.-C. Crasovan, and L. Torner. Three-dimensional spatiotemporal optical solitons in nonlocal nonlinear media. *Phys. Rev. E*, 73:025601(R), 2006.
- [17] D. Mihalache. Multidimensional solitons and vortices in nonlocal nonlinear optical media. *Rom. Rep. Phys.*, 59:515–522, 2007.
- [18] A. Dreischuh, D. N. Neshev, D. E. Petersen, O. Bang, and W. Krolikowski. Observation of attraction between dark solitons. *Phys. Rev. Lett.*, 96:043901, 2006.
- [19] Y. V. Kartashov and L. Torner. Gray spatial solitons in nonlocal nonlinear media. *Opt. Lett.*, 32:946–948, 2007.
- [20] A. Piccardi, A. Alberucci, N. Tabiryan, and G. Assanto. Dark nematicons. *Opt. Lett.*, 36:1356–1358, 2011.
- [21] T. P. Horikis. Small-amplitude defocusing nematicons. *J. Phys. A: Math. Theor.*, 48:02FT01, 2015.
- [22] E. A. Kuznetsov and S. K. Turitsyn. Instability and collapse of solitons in media with a defocusing nonlinearity. *JETP*, 67:1583–1588, 1988.
- [23] D. E. Pelinovsky, Yu. A. Stepanyants, and Yu. S. Kivshar. Self-focusing of plane dark solitons in nonlinear defocusing media. *Phys. Rev. E*, 51:5016–5026, 1995.
- [24] Yu. S. Kivshar and D. E. Pelinovsky. Self-focusing and transverse instabilities of solitary waves. *Phys. Rep.*, 331:117–195, 2000.
- [25] A. Armaroli and S. Trillo. Suppression of transverse instabilities of dark solitons and their dispersive shock waves. *Phys. Rev. A*, 80:053803, 2009.
- [26] G. Assanto. *Nematicons: Spatial Optical Solitons in Nematic Liquid Crystals*. New Jersey: Wiley-Blackwell, 2012.
- [27] G. Assanto, A. A. Minzoni, and N. F. Smyth. Light self-localization in nematic liquid crystals: modelling solitons in nonlocal reorientational media. *J. Nonlinear Opt. Phys. Mater.*, 18:657–691, 2009.
- [28] R. S. Johnson. Water waves and Korteweg-de Vries equations. *J. Fluid Mech.*, 97:701–719, 1980.
- [29] V. I. Karpman. *Non-linear waves in dispersive media*. Elsevier Science & Technology, 1974.
- [30] E. Infeld and G. Rowlands. *Nonlinear waves, solitons and chaos*. Cambridge University Press, 1990.
- [31] R. S. Johnson. *A modern introduction to the mathematical theory of water waves*. Cambridge University Press, 1997.
- [32] M. J. Ablowitz. *Nonlinear dispersive waves: Asymptotic analysis and solitons*. Cambridge University Press, 2011.
- [33] A. Minovich, D. N. Neshev, A. Dreischuh, W. Krolikowski, and Yu. S. Kivshar. Experimental reconstruction of nonlocal response of thermal nonlinear optical media. *Opt. Lett.*, 32:1599–1601, 2007.
- [34] M. Peccianti and G. Assanto. Nematicons. *Phys. Rep.*, 516:147–208, 2012.
- [35] A. Alberucci and G. Assanto. Modeling nematicon propagation. *Mol. Cryst. Liq. Cryst.*, 572:2–12, 2013.
- [36] D. J. Frantzeskakis and B. A. Malomed. Multiscale expansions for a generalized cylindrical nonlinear Schrödinger equation. *Phys. Lett. A*, 264:179–185, 1999.

- [37] M. Remoissenet. *Waves Called Solitons*. Springer, Berlin, 1999.
- [38] D. E. Pelinovsky and Yu. A. Stepanyants. Solitary wave instability in the positive-dispersion media described by the two-dimensional Boussinesq equations. *JETP*, 79:105–112, 1993.
- [39] Yu. S. Kivshar and X. Yang. Ring dark solitons. *Phys. Rev. E*, 50:R40–R43, 1994.
- [40] W. Oevel and W.-H. Steeb. Painleve analysis for a time-dependent Kadomtsev-Petviashvili equation. *Phys. Lett. A*, 103:239–242, 1984.
- [41] K. R. Khusnutdinova, C. Klein, V. B. Matveev, and A. O. Smirnov. On the integrable elliptic cylindrical Kadomtsev-Petviashvili equation. *Chaos*, 23:013126, 2013.
- [42] E. A. Kuznetsov and S. K. Turitsyn. Two- and three-dimensional solitons in weakly dispersive media. *JETP*, 55:844–847, 1982.
- [43] R. Hirota. Exact solutions to the equation describing “cylindrical solitons”. *Phys. Lett. A*, 71:393–394, 1979.
- [44] R. S. Johnson. A note on an asymptotic solution of the cylindrical Korteweg-de Vries equation. *Wave Motion*, 30:1–16, 1999.
- [45] K. Ko and H. H. Kuehl. Cylindrical and spherical Korteweg-deVries solitary waves. *Phys. Fluids*, 22:1343–1348, 1979.
- [46] A. Dreischuh, D. Neshev, G. G. Paulus, F. Grasbon, and H. Walther. Ring dark solitary waves: Experiment versus theory. *Phys. Rev. E*, 66:066611, 2002.
- [47] H. E. Nistazakis, D. J. Frantzeskakis, B. A. Malomed, and P. G. Kevrekidis. Head-on collisions of ring dark solitons. *Phys. Lett. A*, 285:157–164, 2001.
- [48] A. Alberucci, M. Peccianti, G. Assanto, A. Dyadyusha, and M. Kaczmarek. Two-color vector solitons in nonlocal media. *Phys. Rev. Lett.*, 97:153903, 2006.